Thieme

Usefulness of magnifying endoscopy for diagnosis of sessile serrated lesion with dysplasia or carcinoma: Large retrospective study

Authors

Takashi Murakami[1], Eiji Kamba[1], Naoki Tsugawa[1], Hirofumi Fukushima[1], Tomoyoshi Shibuya[1], Takashi Yao[2], Akihito Nagahara[1]

Institutions

1 Gastroenterology, Juntendo University School of Medicine, Tokyo, Japan
2 Human Pathology, Juntendo University School of Medicine, Tokyo, Japan

Keywords

Endoscopy Lower GI Tract, Polyps / adenomas / ..., Colorectal cancer, Diagnosis and imaging (inc chromoendoscopy, NBI, iSCAN, FICE, CLE...)

received 24.1.2024
accepted after revision 27.5.2024
accepted manuscript online 3.6.2024

Bibliography

Endosc Int Open 2024; 12: E895–E904
DOI 10.1055/a-2337-3944
ISSN 2364-3722

Georg Thieme Verlag KG, Rüdigerstraße 14, 70469 Stuttgart, Germany

Corresponding author

Dr. Takashi Murakami, Juntendo University School of Medicine, Gastroenterology, Tokyo, Japan
t-murakm@juntendo.ac.jp

ABSTRACT

Background and study aims Sessile serrated lesions (SSLs) are precursor lesions in the serrated neoplasia pathway that lead to invasive carcinoma from dysplasia arising from SSLs. This study aimed to elucidate the clinicopathological and endoscopic features of SSLs with and without dysplasia or carcinoma.

Patients and methods We reviewed the clinicopathological and endoscopic data from all colorectal lesions pathologically diagnosed as SSLs at Juntendo University Hospital, Tokyo, Japan, between 2011 and 2022. In addition to conventional endoscopic findings, we retrospectively evaluated magnifying endoscopic findings with narrow-band imaging (NBI) or blue laser imaging (BLI) using the Japan NBI Expert Team system and analyzed pit patterns using magnified chromoendoscopic images.

Results Of the 2,132 SSLs, 92.5%, 4.7%, 1.8%, and 0.9% had no dysplasia, low-grade dysplasia, high-grade dysplasia, and submucosal invasive carcinoma, respectively. Older age, the proximal colon, and larger lesions were more frequently associated with SSLs with dysplasia or carcinoma. However, 41.3% of the SSLs with dysplasia or carcinoma were ≤ 10 mm in size. Endoscopic findings, such as (semi) pedunculated morphology, double elevation, central depression, and reddishness, were frequently found in SSLs with dysplasia or carcinoma. Furthermore, magnifying endoscopy using NBI or BLI and magnifying chromoendoscopy showed high sensitivity, specificity, and accuracy for diagnosing dysplasia or carcinoma within SSLs.

Conclusions SSLs with and without dysplasia or carcinoma exhibit distinct clinicopathological and endoscopic features. In an SSL series, conventional endoscopic characteristics in addition to use of magnifying endoscopy may be useful for accurately diagnosing advanced histology within an SSL.

Introduction

Colorectal cancer (CRC) is the third most common cancer and the second leading cause of cancer-related death worldwide [1]. Colonoscopy is used to detect and resect premalignant colorectal polyps; however, 5% to 8% of CRCs are diagnosed in patients who underwent colonoscopy 3 to 5 years earlier [2, 3, 4]. These are called interval cancers or post-colonoscopy CRCs

(PCCRCs) [5] and are a significant concern for physicians. Sessile serrated lesions (SSLs) are thought to be one of the causes of PCCRCs, which occur between completion of colonoscopy and surveillance [2,3]. The 2019 World Health Organization (WHO) Classification of Tumours of the Digestive System has been revised to introduce the term "sessile serrated lesion (SSL)" to replace the previously used term "sessile serrated adenoma/polyp" [6]. SSLs are early precursor lesions of the serrated neoplasia pathway that result in colorectal carcinomas with high levels of microsatellite instability and methylation of DNA repair genes, such as *MLH1*, and *BRAF* mutations [7,8,9,10]. Once SSLs become cancerous, they can rapidly progress to invasive cancers via the serrated tumor pathway [11,12]. Furthermore, with subtle mucosal features similar to those of hyperplastic polyps, SSLs are easily missed and often difficult to diagnose using conventional endoscopy. Such lesions and their rapid malignant progression may be overlooked in relation to development of CRC after colonoscopy.

The serrated neoplasia pathway accounts for up to 30% of CRCs [11,13]. SSL submucosal invasive carcinomas have a higher propensity for lymphatic invasion and lymph node metastasis than conventional adenomas [14], suggesting their high malignancy. Understanding SSL clinicopathological and endoscopic features is crucial. This study aimed to determine the characteristics of SSL-related lesions (including patients with dysplasia or invasive cancer).

Patients and methods

Study design and population

This retrospective study was conducted at Juntendo University Hospital, Tokyo, Japan. From January 2011 to December 2022, 2,177 endoscopically or surgically resected lesions with pathologically diagnosed SSLs with or without dysplasia or cancer were included in the database. During this period, lesions suspected to be SSLs were resected as much as possible, regardless of their size. Nineteen lesions had no colonoscopic images and images from 26 lesions could not be evaluated because of poor quality. Finally, 2,132 lesions (from 1,368 patients) were assessed. This study was approved by the ethics committee of our hospital.

Histological criteria

Histological diagnosis followed the WHO diagnostic criteria for SSLs [6], focusing on features such as crypt serrations, basal crypt dilation, distorted crypts, and growth along the muscularis mucosae. The minimum criterion was presence of at least one architecturally distorted crypt with prominent serrations. Hyperplastic polyps and borderline or indeterminate SSLs were excluded. For SSLs with dysplasia or carcinoma, either a normal SSL component at the lesion edge or an abrupt transition to dysplasia or carcinoma within a single tissue fragment was required. Lesions diagnosed as sessile serrated adenoma/polyp or hyperplastic polyp before 2019 were reviewed based on the 2019 WHO diagnostic criteria for SSLs. All samples were histologically assessed without knowledge of the clinical or endoscopic details. All analyzed specimens were reviewed by one pathologist (T.Y.) with over 30 years of experience in gastrointestinal pathology.

Clinicopathological characteristics

We analyzed clinicopathological characteristics of all patients with lesions, including age, sex, tumor location and size, macroscopic type, and histopathological findings. The proximal colon was defined as the region proximal to the splenic flexure, whereas the remainder of the colon was defined as the distal colon.

Endoscopic analysis

All endoscopic images were obtained using colonoscopes (CF-H260AZI, PCF-Q240ZI, PCF-Q260AZI, CF-H290AZI, or PCF-H290AZI; Olympus Optical, Tokyo, Japan, or EC-L600ZP7; Fujifilm, Tokyo, Japan) with standard video processors (EVIS LUCERA system; Olympus, Tokyo, Japan, or LASEREO; Fujifilm, Tokyo, Japan). Conventional endoscopic findings on white-light colonoscopic images were first evaluated, including the mucus cap, which is considered a strong marker for SSLs. Other endoscopic findings, such as morphology, double elevation, central depression, and reddishness, were also assessed based on a previous report [15]. Macroscopic type was classified according to the Paris-Japanese classification [16]. In particular, (1) pedunculated or semi-pedunculated was defined as the 0-Ip or 0-Isp type in the Paris-Japanese classification [16]; (2) double elevation was defined as a two-step elevation with a clear demarcation; (3) central depression was defined as a clearly depressed area in the center of the lesion; and (4) reddishness was defined as presence of a relatively clear red/pink area compared with adjacent mucosa [15]. Magnification endoscopy with narrow-band imaging (NBI) or blue laser imaging (BLI) was performed to evaluate dark spots inside crypts, indicating crypt dilation, a histological feature of SSLs [17]. The Japan NBI Expert Team (JNET) system [18] was used to evaluate magnifying NBI or BLI endoscopic findings. In addition, pit patterns were investigated using magnified chromoendoscopic images with indigo carmine or crystal violet staining and classified according to Kudo's system [19], including type II open-pit pattern, defined as enlarged star-shaped or round pits [20], which is characteristic of SSLs.

After evaluation, most SSLs (n = 2,121) were endoscopically resected, whereas the remaining SSLs (n = 11) underwent surgical resection. Three experienced endoscopists including two endoscopists (T.M. and H.F.) and one endoscopist (E.K.) with over 15 years and 5 years of experience in colonoscopy, respectively, independently evaluated the images, and discrepancies were resolved by consensus. All images and corresponding lesion data, including patient information and histopathological findings, were collected from the database.

Evaluation of diagnostic ability

We calculated sensitivity, specificity, positive predictive value, negative predictive value, and accuracy for diagnosing SSLs with dysplasia or carcinoma when at least one of the following four markers, including morphology, double elevation, central depression, and reddishness, was found in conventional endo-

▶ **Table 1** Clinicopathological characteristics of studied SSLs.

Variable	ND	LGD	HGD	SIC	Total
n = lesions	**1,972 (92.5%)**	**101 (4.7%)**	**39 (1.8%)**	**20 (0.9%)**	**2,132 (100%)**
(n = patients)	**(1,276)**	**(94)**	**(38)**	(20)	**(1,368)**
Age (years)*	62.8 ± 12.1	64.8 ± 10.0	71.6 ± 8.9	72.2 ± 9.7	63.2 ± 12.0
	(23–91)	(35–85)	(51–86)	(47–90)	(23–91)
Sex					
▪ Male	667 (52.3%)	41 (43.6%)	14 (36.8%)	7 (35.0%)	702 (51.3%)
▪ Female	609 (47.7%)	53 (56.4%)	24 (63.2%)	13 (65.0%)	666 (48.7%)
Location					
▪ Proximal colon	1637 (83.0%)	81 (80.2%)	33 (84.6%)	18 (90.0%)	1769 (83.0%)
▪ Distal colon	335 (17.0%)	20 (19.8%)	6 (15.4%)	2 (10.0%)	363 (17.0%)
Tumor size (mm)†	10.8 ± 7.6	15.0 ± 9.0	14.2 ± 8.4	20.2 ± 12.7	11.1 ± 7.9
	(2–65)	(5–42)	(6–43)	(8–65)	(2–65)

Age and tumor size are presented as mean ± standard deviation (range).
*ND vs. HGD, $P < 0.001$; ND vs. SIC, $P = 0.002$; LGD vs. HGD, $P = 0.002$; and LGD vs. SIC, $P = 0.011$.
† ND vs. LGD, $P < 0.001$; ND vs. HGD, $P = 0.001$; ND vs. SIC, $P < 0.001$; and HGD vs. SIC, $P = 0.049$.
SSL, sessile serrated lesion; ND, no dysplasia; LGD, low-grade dysplasia; HGD, high-grade dysplasia; SIC, submucosal invasive carcinoma.

scopic observation with white light. Similarly, sensitivity, specificity, positive predictive value (PPV), negative predictive value (NPV), and accuracy for diagnosing SSLs with dysplasia or carcinoma were calculated for JNET type 2A, 2B, or 3 lesions (other than type 1) in magnifying NBI or BLI observation, and type III_L, IV, or V pit patterns (other than type II pit pattern) in magnifying chromoendoscopy.

Statistical analyses

Statistical analyses were performed using StatView for Windows version 5.0 (SAS Institute, Inc., Cary, North Carolina, United States). Continuous data were compared using the Mann-Whitney U test. Categorical variables were analyzed using the chi-squared test (with Yates' correction) or Fisher's exact test, as appropriate. Bonferroni's correction was used to compare the differences among three or more groups. $P < 0.05$ was considered statistically significant.

Results

Clinicopathological findings

Clinicopathological characteristics of SSLs are summarized in ▶ **Table 1**. Of the 2,132 SSLs, 92.5% had no dysplasia (ND), 4.7% had low-grade dysplasia (LGD), 1.8% had high-grade dysplasia (HGD), and 0.9% had submucosal invasive carcinoma (SIC). Patients with HGD and SIC were significantly older compared with those with ND and LGD (HGD vs. ND, $P < 0.001$; HGD vs. LGD, $P = 0.002$; SIC vs. ND, $P = 0.002$; SIC vs. LGD, $P = 0.011$). SSLs with dysplasia or carcinoma tended to be more frequently associated with female sex than SSLs without dysplasia, but the difference was not statistically significant. Most lesions in all groups were located in the proximal colon.

Regarding lesion size, a significant stepwise increase in size of the SSL series was identified, along with dysplastic progression from ND to dysplasia to SIC (LGD vs. ND, $P < 0.001$; HGD vs. ND, $P = 0.001$; SIC vs. ND, $P < 0.001$; SIC vs. HGD, $P = 0.049$). Similarly, larger lesions were associated with higher rates of dysplasia or cancer (▶ **Fig. 1**). However, 66 of 160 SSLs (41.3%) with dysplasia or carcinoma were ≤ 10 mm in size.

Endoscopic findings with white light

Endoscopic findings of SSLs are presented in ▶ **Table 2**. Almost all studied lesions (94.5%) were covered with a mucus cap. Macroscopically, 1,881 of NDs (95.4%) were predominantly smooth sessile (0-Is) or superficial type (0-IIa), whereas LGDs, HGDs, and SICs more frequently displayed pedunculated (0-Ip) or semi-pedunculated (0-Isp) morphologies than NDs (LGD and HGD vs. ND, $P < 0.001$; SIC vs. ND, $P = 0.001$). Furthermore, double elevation (0-IIa + Is) was more frequently observed in LGDs, HGDs, and SICs than in NDs (LGD, HGD, and SIC vs. ND, all $P < 0.001$). Regarding central depression (0-IIa + IIc), a similar trend was found between SSLs with dysplasia or carcinoma and those without dysplasia (SIC vs. ND, $P < 0.001$). Reddishness was more frequently observed in LGDs, HGDs, and SICs than in NDs (LGD, HGD, and SIC vs. ND, all $P < 0.001$). In addition, most LGDs, HGDs, and SICs were positive for at least one of four markers, including (semi)pedunculated morphology, double elevation, central depression, and reddishness, compared with NDs ($P < 0.001$).

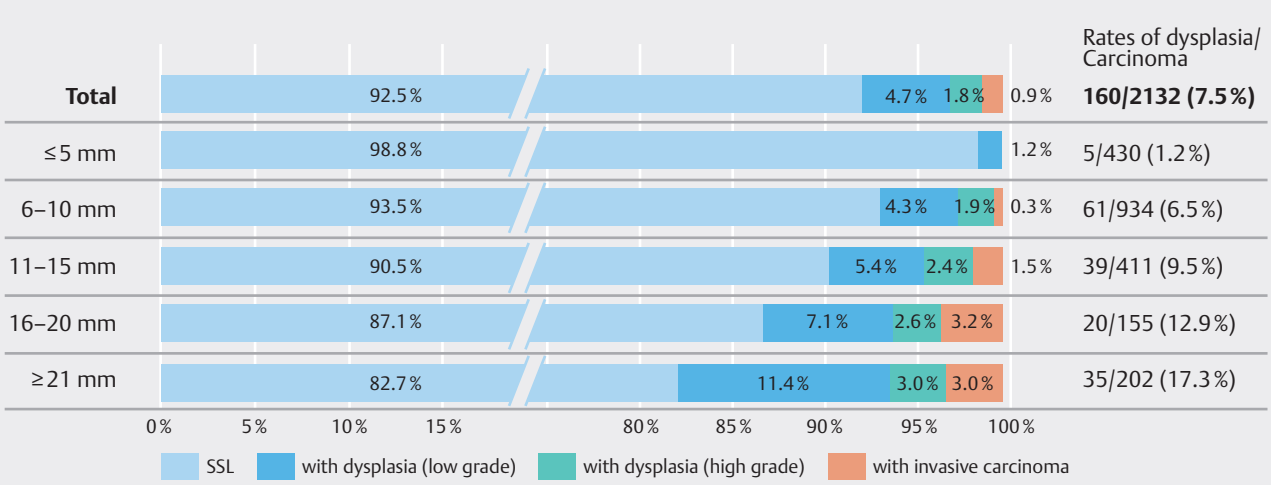

▶ **Fig. 1** Percentage of dysplasia or carcinoma according to size in sessile serrated lesion series. Overall, the rate of dysplasia or carcinoma was 7.5%: 1.2% for lesions ≤ 5 mm, 6.5% for lesions 6 to 10 mm, 9.5% for lesions 11 to 15 mm, 12.9% for lesions 16 to 20 mm, and 17.3% for lesions > 21 mm. Larger lesions were associated with higher rates of dysplasia or carcinoma comorbidities than smaller lesions.

Magnifying endoscopic findings using narrow-band imaging or blue laser imaging

Studied lesions (80.0%) frequently exhibited dark spots inside crypts, which are characteristic of SSLs on image-enhanced endoscopy. According to the JNET classification of magnifying endoscopic findings, all tudied lesions were type 1. In total, 96.9% NDs exhibited type 1 only, whereas 85.2% SSLs with dysplasia or carcinoma had a combination of types 1 and 2A, 2B, or 3, corresponding to SSL and dysplasia or carcinoma, respectively (NDs vs. LGDs, HGDs, and SICs, all $P < 0.001$). Specifically, 78.9% of LGDs had a combination of types 1 and 2A, whereas 33.3% and 46.7% of HGDs had a combination of types 1 and 2A and types 1 and 2B, respectively. Furthermore, no SIC lesions were type 1 only, whereas 56.2% and 31.3% of SICs had a combination of types 1 and 2B and types 1 and 3, respectively (▶ **Table 2**).

Magnifying chromoendoscopic findings

These included 732 NDs, 59 LGDs, 21 HGDs, and 15 SICs. All cases with available images exhibited a type II pit pattern. A type II open pit pattern was found in most lesions in all the groups, with no statistical significance. In total, 721 NDs (98.5%) exhibited a type II pit pattern only, whereas 83 SSLs (87.4%) with dysplasia or carcinoma had a combination of type II and III_L, IV, or V pit patterns, corresponding to SSL and dysplasia or carcinoma, respectively (NDs vs. LGDs, HGDs, and SICs, all $P < 0.001$). Forty-nine LGDs (83.1%) had a combination of types II and III_L or IV pit patterns, and seven (33.4%) and 12 HGDs (57.1%) had a combination of type II + III_L or IV pit patterns and of type II + V pit patterns, respectively. Furthermore, no SIC lesions showed a type II pit pattern only, whereas 12 (80.0%) SICs had a combination of type II and V pit patterns (▶ **Table 2**).

Sensitivity, specificity, positive and negative predictive values, and accuracy for sessile serrated lesions using magnifying endoscopy

▶ **Table 3** shows sensitivity, specificity, PPV, NPV, and accuracy for identifying SSLs with dysplasia or carcinoma. Presence of at least one of four markers, including (semi)pedunculated morphology, double elevation, central depression, and reddishness, had a sensitivity of 81.9% (95% confidence interval [CI] 75.7–86.9) and a specificity of 89.7% (95% CI 89.2–90.1). Combining types 1 and 2A, 2B, or 3 of the JNET classification by magnifying NBI or BLI endoscopy resulted in higher sensitivity (85.2%; 95% CI 79.1–90.0), specificity (96.9%; 95% CI 96.4–97.3), NPV (98.8%; 95% CI 98.3–99.2), and overall diagnostic accuracy (96.0%; 95% CI 95.1–96.7). Similarly, combining type II and III_L, IV, V_I, or V_N pit patterns using magnifying endoscopy resulted in high sensitivity (87.4%; 95% CI 81.7–91.3), specificity (98.5%; 95% CI, 97.8–99.0), NPV (98.4%; 95% CI 97.6–98.9), and overall diagnostic accuracy (97.2%; 95% CI, 95.9–98.1).

Representative endoscopic images of SSLs with dysplasia and invasive carcinoma are shown in ▶ **Fig. 2** and ▶ **Fig. 3**, respectively.

Discussion

This study shows that conventional endoscopic characteristics along with use of magnifying endoscopy may be useful for accurately diagnosing SSLs with dysplasia or carcinoma. Limited studies have objectively evaluated the effectiveness of magnifying endoscopic findings in SSLs with dysplasia or carcinoma. Although we previously reported on endoscopic findings for diagnosing SSLs with dysplasia or carcinoma [15], that research was based on a relatively small number of cases. Another study by Enomoto et al. showed that visible vessels observed using magnifying NBI could indicate SSLs with cancerous components [21]. However, their analysis was limited by presence or

▶ **Table 2** Endoscopic characteristics of studied SSLs.

Variable	ND	LGD	HGD	SIC	Total
Conventional endoscopy					
n = lesions	**1,972**	**101**	**39**	**20**	**2,132**
Mucus cap	1,868 (94.7%)	91 (90.1%)	37 (94.9%)	19 (95.0%)	2,015 (94.5%)
▪ (a) (Semi)pedunculated morphology (0-Ip or 0-Isp)*[a]	51 (2.6%)	14 (13.9%)*	10 (25.6%)*	5 (25.0%)*	80 (3.8%)
▪ (b) Double elevation (0-IIa + Is)*[b]	70 (3.5%)	61 (60.4%)*	19 (48.7%)*	10 (50.0%)*	160 (7.5%)
▪ (c) Central depression (0-IIa + IIc)*[c]	44 (2.2%)	6 (5.9%)*	2 (5.1%)	6 (30.0%)*	58 (2.7%)
▪ (d) Reddishness*[d]	77 (3.9%)	40 (39.6%)*	21 (53.8%)*	16 (80.0%)*	154 (7.2%)
At least one of the four markers, including (a), (b), (c), and (d)*	204 (10.3%)	79 (78.2%)*	33 (84.6%)*	19 (95.0%)*	335 (15.7%)
Magnifying NBI or BLI					
n = lesions	**1,542**	**76**	**30**	**16**	**1,664**
Dark spots	1,249 (81.0%)	54 (71.1%)	20 (66.7%)	8 (50.0%)	1,331 (80.0%)
JNET classification**					
▪ Type 1 only	1,494 (96.9%)	13 (17.1%)	5 (16.7%)	–	1,512 (90.9%)
▪ Type 1 + 2A	48 (3.1%)	60 (78.9%)	10 (33.3%)	2 (12.5%)	120 (7.2%)
▪ Type 1 + 2B	–	3 (4.0%)	14 (46.7%)	9 (56.2%)	26 (1.6%)
▪ Type 1 + 3	–	–	1 (3.3%)	5 (31.3%)	6 (0.3%)
Magnifying chromoendoscopy					
n = lesions	**732**	**59**	**21**	**15**	**827**
Type II open pit pattern	627 (85.7%)	46 (78.0%)	19 (90.5%)	11 (73.3%)	703 (85.0%)
Pit pattern classification***					
▪ Type II only	721 (98.5%)	10 (16.9%)	2 (9.5%)	–	733 (88.6%)
▪ Type II + III_L	7 (1.0%)	20 (33.9%)	4 (19.1%)	–	31 (3.8%)
▪ Type II + IV	4 (0.5%)	29 (49.2%)	3 (14.3%)	3 (20.0%)	39 (4.7%)
▪ Type II + V_I	–	–	12 (57.1%)	6 (40.0%)	18 (2.2%)
▪ Type II + V_N	–	–	–	6 (40.0%)	6 (0.7%)

A total of 1,664 lesions and 827 lesions were evaluated for NBI or BLI magnifying endoscopic and magnifying chromoendoscopic findings, respectively. In JNET and pit pattern classifications, the largest one is shown. For example, type II + V_I pit patterns include lesions showing type II and V_I pit patterns, with or without type III and IV pit patterns.

* [a] ND vs. LGD, $P < 0.001$; ND vs. HGD, $P < 0.001$; and ND vs. SIC, $P = 0.001$

* [b] ND vs. LGD, $P < 0.001$; ND vs. HGD, $P < 0.001$; and ND vs. SIC, $P < 0.001$

* [c] ND vs. SIC, $P < 0.001$; and LGD vs. SIC, $P = 0.029$

* [d] ND vs. LGD, $P < 0.001$; ND vs. HGD, $P < 0.001$; ND vs. SIC, $P < 0.001$; and LGD vs. SIC, $P = 0.007$

*ND vs. LGD, $P < 0.001$; ND vs. HGD, $P < 0.001$; and ND vs. SIC, $P < 0.001$

**ND vs. LGD, $P < 0.001$; ND vs. HGD, $P < 0.001$; ND vs. SIC, $P < 0.001$; LGD vs. HGD, $P<0.001$; and LGD vs. SIC, $P < 0.001$

***ND vs. LGD, $P<0.001$; ND vs. HGD, $P < 0.001$; ND vs. SIC, $P < 0.001$; LGD vs. HGD, $P < 0.001$; and LGD vs. SIC, $P < 0.001$

SSL, sessile serrated lesion; ND, no dysplasia; LGD, low-grade dysplasia; HGD, high-grade dysplasia; SIC, submucosal invasive carcinoma; NBI, narrow-band imaging; BLI, blue laser imaging; JNET, Japan NBI Expert Team.

absence of visible vessels and a small number of cases. The strength of this study lies in the large number of colorectal SSL cases analyzed and detailed evaluation of magnifying endoscopic findings.

Among SSLs, 92.5%, 4.7%, 1.8%, and 0.9% lesions had ND, LGD, HGD, and SIC, respectively. A previous study reported that frequencies of dysplasia and invasive carcinoma among SSLs were 14% and 1.0%, respectively [22]. Another study found three HGDs (0.7%) and one SIC (0.2%) among 430 SSLs [23]. The slight variation in dysplasia frequency may stem from differences in histopathological diagnostic criteria. SIC frequency in this study was generally consistent with that of previous reports.

▶ **Table 3** Sensitivity, specificity, positive and negative predictive values, and overall diagnostic accuracy for identifying SSLs with dysplasia or carcinoma.

	Sensitivity (%)	Specificity (%)	Positive predictive value (%)	Negative predictive value (%)	Overall diagnostic accuracy (%)
Presence of at least one of the four markers, including (semi)pedunculated morphology, double elevation, central depression, and reddishness	81.9	89.7	39.1	98.4	89.1
	(75.7–86.9)	(89.2–90.1)	(36.1–41.5)	(97.8–98.8)	(88.1–89.8)
Combining JNET types 1 and 2A, 2B, or 3 using magnifying NBI or BLI	85.2	96.9	68.4	98.8	96.0
	(79.1–90.0)	(96.4–97.3)	(63.5–72.2)	(98.3–99.2)	(95.1–96.7)
Combining types II and III_L, IV, V_I, or V_N pit patterns using magnifying chromoendoscopy	87.4	98.5	88.3	98.4	97.2
	(81.7–91.3)	(97.8–99.0)	(82.6–92.3)	(97.6–98.9)	(95.9–98.1)

Values are presented as means (95% confidence intervals).

Clinicopathologically, SSLs with dysplasia or carcinoma were associated with older women more than those with ND, without significant sex distinction in this study, which aligns with previous reports [14, 15]. Advanced histological features, such as tubulovillous changes or HGD, are more prevalent in larger polyps than in smaller polyps [24, 25]. In addition, larger polyps often carry an increased risk of associated carcinoma. This analysis also revealed a correlation between SSL size and dysplasia or carcinoma comorbidities, with larger SSLs exhibiting higher comorbidity rates. Notably, more than 40% of SSLs with dysplasia or carcinoma were ≤ 10 mm in size. Goldstein [12] found that median size of eight SSLs with focal invasive adenocarcinomas or HGD was 8.5 mm (range, 6–12 mm). Another study [26] showed that among eight SSLs with intramucosal, submucosal, or advanced carcinomas, the largest diameter was ≤ 10 mm. These findings suggest that even small SSLs may be at risk of dysplasia or carcinoma.

SSLs are often covered by a thin layer called a "mucus cap," and they are more commonly found in the proximal colon [10, 27, 28]. In this study, most SSLs showed mucus adhesion, which is consistent with previous reports. Mucus adhesion in the proximal colon can be useful evidence for identifying SSLs. Furthermore, SSLs with dysplasia may not always show a simple whitish, flat-elevated morphology. Nanda et al. [29] reported that SSLs with dysplasia had two distinct morphological areas meeting at an endoscopically apparent transition point. In a previous study [15], (semi)pedunculated morphologies, double elevations, central depressions, and reddishness were more common in SSLs with dysplasia or carcinoma than in those without, which is consistent with our findings.

However, diagnosing SSLs with dysplasia or carcinoma can be challenging using conventional white-light endoscopy alone. Image-enhanced endoscopy techniques, such as NBI or BLI, can enhance diagnosis of these subtle lesions [30, 31, 32]. Several studies have demonstrated clinical usefulness of the JNET classification for conventional colorectal lesions [33, 34]. In this study, all lesions exhibited JNET type 1, suggesting that histological characteristics of SSLs resemble those of hyperplastic polyps lacking expanded vascularity. In addition, the lesions frequently showed dark spots inside the crypts, a feature often revealed by NBI, indicating crypt dilation, which is consistent with our findings. Presence of JNET type 1 and dark spots inside the crypts may aid endoscopists in diagnosing SSLs during colonoscopy.

A detailed analysis of the JNET classification revealed that lesions classified as JNET type 2A in our study were mostly non-dysplastic, dysplastic, or shallow SICs, with only one case of deep SIC. Therefore, JNET type 2A SSLs can be endoscopically treated because of their low risk of lymph node metastasis. Lesions classified as JNET type 2B included various histological features, such as SSL with LGD, HGD, and invasive carcinoma, consistent with results of previous studies [33, 34]. Dysplastic or shallow invasive cancers can be endoscopically treated because of their low risk of lymph node metastasis, whereas deep invasive cancers usually require surgical resection with lymph node dissection because of their higher risk of lymph node metastasis. Therefore, accurate qualitative and quantitative diagnoses of SSLs with dysplasia or invasive carcinoma are crucial for determining treatment strategies. Differentiating among dysplasia, shallow SIC, and deep SIC in SSLs diagnosed as JNET type 2B is challenging. Performing an additional pit pattern procedure using magnifying chromoendoscopy can aid in accurate diagnosis. Conversely, five of six lesions classified as JNET type 3 were deep SICs in our study, consistent with previous reports [33, 34], indicating that JNET type 3 may be associated with deep SIC in SSLs. These lesions are associated with a high risk of lymph node metastasis and should be considered for surgical intervention.

In colonoscopy, the significance of performing a pit pattern diagnosis in addition to NBI or BLI findings lies in its ability to evaluate microscopic morphology of tissues, enabling more accurate assessment of lesions. The pit pattern classification of colorectal lesions by Kudo et al. [19] correlates with their histological characteristics and is valuable for distinguishing neoplastic from non-neoplastic lesions and assessing the depth of invasion in early CRCs [19, 35]. Recently, a type II open-pit pattern has been identified as a hallmark of SSLs [20]. In this study, SSLs with magnified images mostly exhibited a type II open pat-

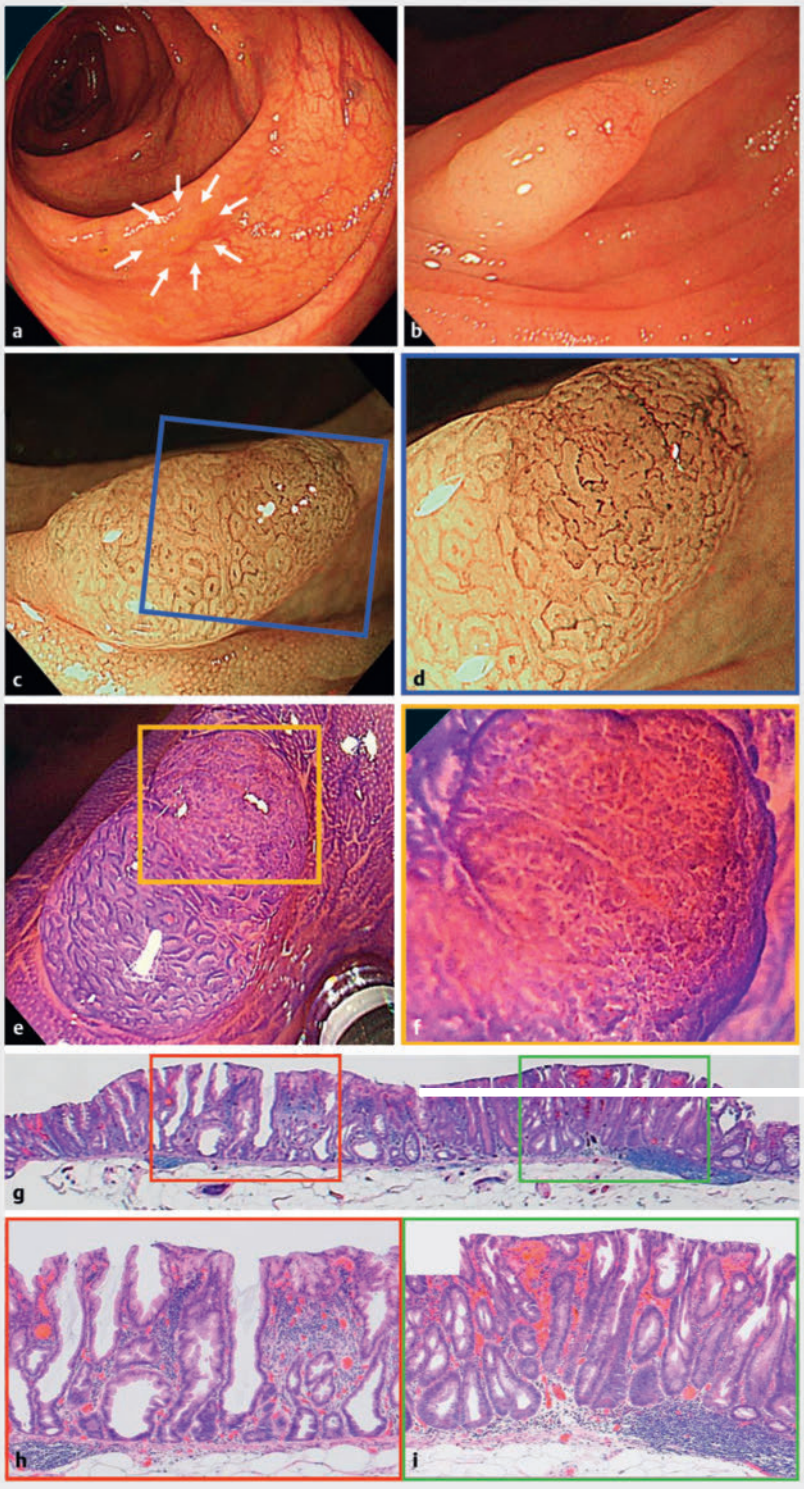

▶ **Fig. 2** Endoscopic images of a sessile serrated lesion (SSL) with dysplasia in a representative case. **a** A 67-year-old man. Conventional endoscopy shows a 6-mm-sized 0-Is type lesion in the transverse colon (white arrows). **b** A little closer view. A white area on the left side and a reddish area on the right can be observed. **c, d** Narrow-band imaging (NBI) magnification reveals dark spots characteristic of SSL, Japan NBI Expert Team (JNET) type 1, in the white area, whereas irregular vascular structures corresponding to JNET type 2B are observed in the reddish area. **e, f** Magnified observation under crystal violet staining reveals type II open pit pattern in the white area, whereas a V_I-mild pit pattern is observed in the reddish area. **g** Low-power field view of the resected specimen. **h** Higher-power field view of the red square in **g**. Crypts with a serrated architecture exhibit irregularly dilated crypts and horizontally arranged basal crypts, corresponding to SSL. **i** Higher-power field view of the green square in **g**. A histopathological image shows conventional adenomatous low- to high-grade dysplasia with cytological atypia and architectural dysplasia in the nodular area. The lesion is pathologically consistent with SSL with high-grade dysplasia.

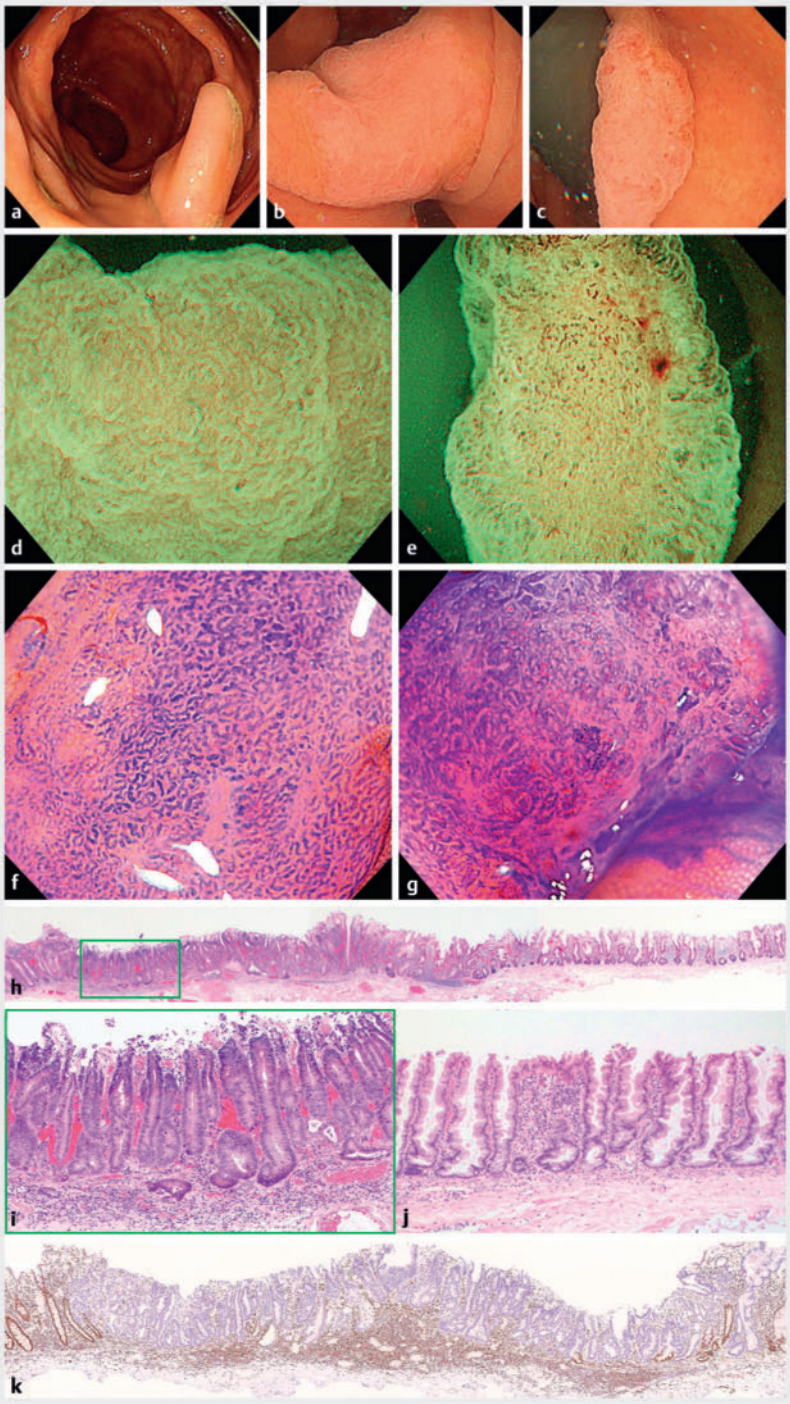

▶ **Fig. 3** Endoscopic images of an invasive submucosal carcinoma arising from sessile serrated lesion in a representative case. **a** An 84-year-old woman. Conventional endoscopy shows an elevated lesion with rich mucus 20 mm in diameter at the ascending colon. **b** After carefully washing away the mucus, a flat-elevated lesion with faded color can be observed. **c** A retroflex view is shown. A clear depressed area is observed on the oral side of the lesion. **d** Magnifying narrow-band imaging (NBI) shows an invisible vessel pattern in the anal side of the lesion, classified as Japan NBI Expert Team (JNET) type 1. **e** Magnifying NBI in retroflex view shows an irregular vessel and surface pattern, classified as JNET type 2B, in an oral of the lesion. **f** Magnifying chromoendoscopy using crystal violet staining shows a type II open pit pattern in the anal side of the lesion. **g** Magnifying chromoendoscopy in retroflex view shows type V_I-mild pit pattern consisting of areas with irregular pits in an oral of the lesion. We endoscopically diagnosed the lesion as a sessile serrated lesion (SSL) with dysplasia or shallow invasive submucosal carcinoma arising from SSL and achieved an en bloc resection by performing an endoscopic submucosal dissection. **h, i, j** Histopathological findings with hematoxylin-eosin staining of the resected specimen. **h** Low-power field view of the resected specimen. **i** Higher-power field view of the green square in **h**. Well-differentiated adenocarcinomas slightly invade the submucosa. **j** Crypts with a serrated architecture exhibit irregularly dilated crypts, irregularly branching crypts, and horizontally arranged basal crypts, corresponding to SSL. The adenocarcinoma component is histologically continuous with SSL. **k** Immunostaining of hMLH1 of adenocarcinoma. Loss of hMLH1 expression is shown preferentially in the tumor area. Therefore, this lesion was pathologically consistent with a submucosal invasive adenocarcinoma associated with an SSL.

tern. Most SSLs without dysplasia had only a type II pit pattern, whereas SSLs with dysplasia or carcinoma showed a mix of type II and other patterns, such as III_L, IV, V_I, or V_N. Among lesions diagnosed with type III or IV pit patterns, 80.0% were SSLs with dysplasia, indicating an adenoma-like appearance that may be suitable for endoscopic treatment. Similarly, most lesions with a type V_I-mild pit pattern were SSLs with HGD or shallow invasive submucosal carcinoma, suggesting a low risk of lymph node metastasis and suitability for endoscopic treatment. Conversely, most lesions with V_I-severe or V_N pit patterns are deep, invasive, submucosal carcinomas, indicating need for surgical resection. Therefore, magnifying the endoscopic pit pattern is effective for assessing depth of invasion in early cancer from SSLs. Magnifying chromoendoscopy may provide valuable guidance in selecting between endoscopic and surgical resection of SSLs with dysplasia or carcinoma.

Presence of at least one of these four markers, including (semi) pedunculated morphology, double elevation, central depression, and reddishness, had a high sensitivity (81.9%), specificity (89.7%), and overall diagnostic accuracy (89.1%) for identification of SSLs with dysplasia or carcinoma. These findings corroborate our previous report [15], suggesting that endoscopic characteristics, including the four markers, may be useful for accurately diagnosing SSLs with advanced histology. Furthermore, sensitivity, specificity, and overall diagnostic accuracy for identification of SSLs with dysplasia or carcinoma using magnifying endoscopy, such as NBI or BLI or chromoendoscopy, were higher than those using white light. According to results of our analysis, we strongly recommend that if at least one of the four markers, including (semi)pedunculated morphology, double elevation, central depression, and reddishness, is found in SSLs on conventional endoscopy, magnifying endoscopy should be used in evaluation.

This study had some limitations. First, there may have been bias in specimen selection, because the materials included colorectal lesions resected endoscopically or surgically and diagnosed as SSLs in a retrospective analysis conducted at a single center. Second, the sample size of SSLs with dysplasia or carcinoma was small owing to their rarity, although this study examined a larger number of cases than previous studies. Third, some patients had low-quality endoscopic images, which affected precise evaluation of endoscopic features. Fourth, this study did not analyze interobserver and intraobserver variabilities in interpretation of endoscopic findings. Finally, magnifying endoscopic findings were evaluated after conventional endoscopic diagnosis, potentially influencing reviewer assessment. Further studies are required to better understand clinicopathological and endoscopic characteristics of dysplasia or carcinoma arising from SSLs and confirm their clinical utility.

Conclusions

In conclusion, our findings suggest that SSLs with dysplasia or carcinoma may be more common in older individuals, located in the proximal colon, and larger in size. However, dysplasia and cancer can coexist in SSLs even when they are ≤ 10 mm. In addition, endoscopic characteristics, such as (semi)pedunculated morphology, reddishness, double elevation, central depression, and magnifying endoscopic findings such as JNET type 2A, 2B, or 3, or III_L, IV, V_I, or V_N pit patterns, may aid in accurate diagnosis of SSLs with dysplasia or carcinoma. These findings may help improve identification and complete resection of SSLs with dysplasia or invasive carcinoma, ultimately reducing CRC rates.

Conflict of Interest

The authors declare that they have no conflict of interest.

References

[1] Sung H, Ferlay J, Siegel RL et al. Global cancer statistics 2020: GLOBOCAN estimates of incidence and mortality worldwide for 36 cancers in 185 countries. CA Cancer J Clin 2021; 71: 209–249 doi:10.3322/caac.21660

[2] Arain MA, Sawhney M, Sheikh S et al. CIMP status of interval colon cancers: another piece to the puzzle. Am J Gastroenterol 2010; 105: 1189–1195

[3] Cooper GS, Xu F, Barnholtz Sloan JS et al. Prevalence and predictors of interval colorectal cancers in medicare beneficiaries. Cancer 2012; 118: 3044–3052

[4] Anderson R, Burr NE, Valori R. Causes of post-colonoscopy colorectal cancers based on World Endoscopy Organization System of Analysis. Gastroenterology 2020; 158: 1287–1299 doi:10.1053/j.gastro.2019.12.031

[5] Rutter MD, Beintaris I, Valori R et al. World endoscopy organization consensus statements on post-colonoscopy and post-imaging colorectal cancer. Gastroenterology 2018; 155: 909–925 doi:10.1053/j.gastro.2018.05.038

[6] Pai RK, Mäkinen MJ, Rosty C. Colorectal serrated lesions and polyps. In: Nagtegaal ID, Arends MJ, Odze RD (eds.) WHO Classification of Tumours of the Digestive System, 5th edn. et al. Lyon: IARC Press; 2019: 163–169

[7] O'Brien MJ, Yang S, Mack C et al. Comparison of microsatellite instability, CpG island methylation phenotype, BRAF and KRAS status in serrated polyps and traditional adenomas indicates separate pathways to distinct colorectal carcinoma end points. Am J Surg Pathol 2006; 30: 1491–1501 doi:10.1097/01.pas.0000213313.36306.85

[8] Patil DT, Shadrach BL, Rybicki LA et al. Proximal colon cancers and the serrated pathway: a systematic analysis of precursor histology and BRAF mutation status. Mod Pathol 2012; 25: 1423–1431 doi:10.1038/modpathol.2012.98

[9] Murakami T, Mitomi H, Saito T et al. Distinct WNT/β-catenin signaling activation in the serrated neoplasia pathway and the adenoma-carcinoma sequence of the colorectum. Mod Pathol 2015; 28: 146–158 doi:10.1038/modpathol.2014.41

[10] Spring KJ, Zhao ZZ, Karamatic R et al. High prevalence of sessile serrated adenomas with BRAF mutations: a prospective study of patients undergoing colonoscopy. Gastroenterology 2006; 131: 1400–1407

[11] Snover DC. Update on the serrated pathway to colorectal carcinoma. Hum Pathol 2011; 42: 1–10 doi:10.1016/j.humpath.2010.06.002

[12] Goldstein NS. Small colonic microsatellite unstable adenocarcinomas and high-grade epithelial dysplasias in sessile serrated adenoma polypectomy specimens: a study of eight cases. Am J Clin Pathol 2006; 125: 132–145

[13] Jass JR. Classification of colorectal cancer based on correlation of clinical, morphological and molecular features. Histopathology 2007; 50: 113–130 doi:10.1111/j.1365-2559.2006.02549.x

[14] Murakami T, Mitomi H, Yao T et al. Distinct histopathological characteristics in colorectal submucosal invasive carcinoma arising in sessile serrated adenoma/polyp and conventional tubular adenoma. Virchows Arch 2018; 472: 383–393 doi:10.1007/s00428-017-2234-8

[15] Murakami T, Sakamoto N, Ritsuno H et al. Distinct endoscopic characteristics of sessile serrated adenoma/polyp with and without dysplasia/carcinoma. Gastrointest Endosc 2017; 85: 590–600

[16] Kudo SE, Lambert R, Allen JI et al. Nonpolypoid neoplastic lesions of the colorectal mucosa. Gastrointest Endosc 2008; 68: S3–S47 doi:10.1016/j.gie.2008.07.052

[17] Hazewinkel Y, López-Cerón M, East JE et al. Endoscopic features of sessile serrated adenomas: validation by international experts using high-resolution white-light endoscopy and narrow-band imaging. Gastrointest Endosc 2013; 77: 916–924 doi:10.1016/j.gie.2012.12.018

[18] Sano Y, Tanaka S, Kudo SE et al. Narrow-band imaging (NBI) magnifying endoscopic classification of colorectal tumors proposed by the Japan NBI Expert Team. Dig Endosc 2016; 28: 526–533 doi:10.1111/den.12644

[19] Kudo S, Tamura S, Nakajima T et al. Diagnosis of colorectal tumorous lesions by magnifying endoscopy. Gastrointest Endosc 1996; 44: 8–14 doi:10.1016/s0016-5107(96)70222-5

[20] Kimura T, Yamamoto E, Yamano HO et al. A novel pit pattern identifies the precursor of colorectal cancer derived from sessile serrated adenoma. Am J Gastroenterol 2012; 107: 460–469

[21] Enomoto Y, Ishioka M, Chino A et al. Advantage of magnifying narrow-band imaging for the diagnosis of colorectal neoplasia associated with sessile serrated lesions. DEN Open 2023; 4: e315

[22] Lash RH, Genta RM, Schuler CM. Sessile serrated adenomas: prevalence of dysplasia and carcinoma in 2139 patients. J Clin Pathol 2010; 63: 681–686 doi:10.1136/jcp.2010.075507

[23] Chino A, Yamamoto N, Kato Y et al. The frequency of early colorectal cancer derived from sessile serrated adenoma/polyps among 1858 serrated polyps from a single institution. Int J Colorectal Dis 2016; 31: 343–349

[24] Hassan C, Pickhardt PJ, Kim DH et al. Systematic review: distribution of advanced neoplasia according to polyp size at screening colonoscopy. Aliment Pharmacol Ther 2010; 31: 210–217 doi:10.1111/j.1365-2036.2009.04160.x

[25] Turner KO, Genta RM, Sonnenberg A. Lesions of all types exist in colon polyps of all sizes. Am J Gastroenterol 2018; 113: 303–306 doi:10.1038/ajg.2017.439

[26] Ban S, Mitomi H, Horiguchi H et al. Adenocarcinoma arising in small sessile serrated adenoma/polyp (SSA/P) of the colon: clinicopathological study of eight lesions. Pathol Int 2014; 64: 123–132 doi:10.1111/pin.12147

[27] Tadepalli US, Feihel D, Miller KM et al. A morphologic analysis of sessile serrated polyps observed during routine colonoscopy (with video). Gastrointest Endosc 2011; 74: 1360–1368

[28] Gurudu SR, Heigh RI, De Petris G et al. Sessile serrated adenomas: demographic, endoscopic and pathological characteristics. World J Gastroenterol 2010; 16: 3402–3405 doi:10.3748/wjg.v16.i27.3402

[29] Nanda KS, Tutticci N, Burgess N et al. Caught in the act: endoscopic characterization of sessile serrated adenomas with dysplasia. Gastrointest Endosc 2014; 79: 864–870

[30] Hirata M, Tanaka S, Oka S et al. Magnifying endoscopy with narrow band imaging for diagnosis of colorectal tumors. Gastrointest Endosc 2007; 65: 988–995

[31] East JE, Suzuki N, Bassett P et al. Narrow band imaging with magnification for the characterization of small and diminutive colonic polyps: Pit pattern and vascular pattern intensity. Endoscopy 2008; 40: 811–817

[32] Yoshida N, Yagi N, Inada Y et al. Ability of a novel blue laser imaging system for the diagnosis of colorectal polyps. Dig Endosc 2014; 26: 250–258 doi:10.1111/den.12127

[33] Iwatate M, Sano Y, Tanaka S et al. Validation study for development of the Japan NBI Expert Team classification of colorectal lesions. Dig Endosc 2018; 30: 642–651 doi:10.1111/den.13065

[34] Sumimoto K, Tanaka S, Shigita K et al. Clinical impact and characteristics of the narrow-band imaging magnifying endoscopic classification of colorectal tumors proposed by the Japan NBI Expert Team. Gastrointest Endosc 2017; 85: 816–821 doi:10.1016/j.gie.2016.07.035

[35] Kudo S, Rubio CA, Teixeira CR et al. Pit pattern in colorectal neoplasia: endoscopic magnifying view. Endoscopy 2001; 33: 367–373 doi:10.1055/s-2004-826104